Journal of Mathematical Modeling
Vol. 8, No. 2, 2020, pp. 177–188

JMM

Finite difference method for capillary formation model in tumor angiogenesis

Amin Shahkarami* **, Bahman Ghazanfari**

Department of Mathematics, Lorestan University, Khorramabad, Iran

Email(s): shahkarami67@gmail.com, ghazanfari.ba@lu.ac.ir

Abstract. An implicit finite difference method is implied to approximate a parabolic partial differential equation for capillary formation in tumor angiogenesis. After that, the stability analysis of the method will be investigated. At the end, some numerical simulations are considered to show the applicability and efficiency of the scheme.

Keywords: Parabolic partial differential equations, tumor angiogenesis, finite difference method, stability analysis.
AMS Subject Classification 2010: 65N06, 92B05.

1 Introduction

Mathematical methods can help scientists to find solutions of problems. There are many types of research to imply methodology for mathematical models. We can point out the novel biological problems like [3,4]. Although there are many mathematical models, the capillary formation model in tumor angiogenesis is the one we address in this paper.

Angiogenesis is a natural phenomenon meaning the formation of new capillaries from the previous vessels and plays an important role in various physiological processes such as organ development, wound healing and reproduction. However, the internal conditions of the body sometimes cause excessive proliferation of this phenomenon causing the formation of a local tumor.

*Corresponding author.
Received: 26 February 2020 / Revised: 17 March 2020 / Accepted: 17 March 2020.
DOI: 10.22124/jmm.2020.15830.1386

© 2020 University of Guilan

A mathematical model for capillary formation in tumor angiogenesis is presented as [1, 2, 5–7]

$$\begin{aligned}
&\frac{\partial u}{\partial t} = \mathcal{K}\frac{\partial}{\partial x}\Big(u\frac{\partial}{\partial x}\big(\ln\frac{u}{h(x)}\big)\Big), \qquad 0 < x < 1, \quad 0 < t \le \tau,\\
&u(x,0) = 1, \qquad 0 < x < 1,\\
&\mathcal{K}u\frac{\partial}{\partial x}\big(\ln\frac{u}{h(x)}\big)\big|_{x=0} = 0, \qquad 0 \le t \le \tau,\\
&\mathcal{K}u\frac{\partial}{\partial x}\big(\ln\frac{u}{h(x)}\big)\big|_{x=1} = 0, \qquad 0 \le t \le \tau,
\end{aligned} \tag{1}$$

where $u(x,t)$ represents the concentration of endothelial cells and describes the motion of endothelial cells with the cell diffusion constant $\mathcal{K}$, which is chosen as a non-zero constant [1, 2, 6, 7] and h is named the transition probability function which is defined by

$$h(x) = \Big(\frac{a + Ax^s(1-x)^s}{b + Ax^s(1-x)^s}\Big)^{\beta_1}\Big(\frac{d+1-Bx^s(1-x)^s}{d+1-Bx^s(1-x)^s}\Big)^{\beta_2}.$$

Moreover, the parameters a, b, d, e, A, B, s, β_1, and β_2 are some arbitrary constants [1, 2, 5–7].

By setting $H(x) = h'(x)/h(x)$ we get

$$\frac{\partial}{\partial x}\Big(\ln\frac{u}{h(x)}\Big) = \frac{u_x}{u} - \frac{h'(x)}{h(x)} = \frac{u_x}{u} - H(x),$$

so that

$$u\frac{\partial}{\partial x}\big(\ln\frac{u}{h(x)}\big) = u\big(\frac{u_x}{u} - H(x)\big) = u_x - uH(x),$$

and therefore

$$\frac{\partial u}{\partial t} = \mathcal{K}\Big(u_{xx} - \frac{\partial}{\partial x}\big(uH(x)\big)\Big). \tag{2}$$

Similarly, for boundary conditions, we obtain

$$\begin{aligned}
&\frac{\partial}{\partial x}u\big|_{x=0} - u(0,t)H(0) = 0, \qquad 0 \le t \le \tau,\\
&\frac{\partial}{\partial x}u\big|_{x=1} - u(1,t)H(1) = 0, \qquad 0 \le t \le \tau.
\end{aligned} \tag{3}$$

Different numerical methods have been proposed to solve the above model. The first method is to use the method of lines presented by Pumak and Erdem [6]. This method, first, converts the partial differential equation (PDE) (1) to a system of ordinary differential equations (ODEs), and then

solves this system of ODEs [6]. Saadatmandi et al. in [7] implemented a method based on the shifted Legendre polynomials. The iterated operating method was published by the authors of [2]. This method, firstly, splits the equations into two parts, then it applies suitable difference approximation techniques for each part to obtain linear bounded systems. At the end, these systems are combined with iterative schemes and the midpoint rule [2]. Finally, Abbasbandy et al. applied an analysis based on radial basis functions meshfree method for the problem [1].

To obtain stable numerical solutions, the authors in the first three methods set the value of the cell diffusion constant, $\mathcal{K}$, in some small values. However, this restriction was neglected in applying the fourth method [2].

Unfortunately, the stability of the RBF method depends on an extra parameter called the shape parameter and this makes the stability false for either the RBF type or some values of the shape parameter.

In the RBF method, the model was approximated by a weighted iterated method based on two levels n and $n+1$ for interior domain, and an approximation based on level $n+1$ for boundary points. In this paper, we apply a weighted finite difference (FD) method for all points of the spatial domain at one time level.

The finite difference method is presented in Section 2 and the stability analysis of the FD method is discussed in Section 3. Finally, some numerical simulations and the conclusion are presented in Section 4 and Section 5, respectively.

2 Finite difference method

The purpose of this section is to present a weighted approximating solution of (2)-(3) between two consecutive time levels n and $n+1$ based on the finite difference method. To this end, we impose $0 \leq \theta \leq 1$ and partition the interval $[0,1]$ by N points as $\{x_k = k\Delta x : k = 1, 2, \ldots, N\}$ and the interval $[0,\tau]$ by $m+1$ points as $\{t_n = n\Delta t : n = 0, 1, \ldots, m\}$ where $\Delta x = \frac{1}{N}$ and $\Delta t = \frac{\tau}{m+1}$.

The aim is to attain a numerical solution at time level $n+\theta$. Hence, we try to approximate (2)-(3) as

$$\frac{\partial u}{\partial t}\Big|_k^{n+\theta} = \mathcal{K}\Big(\frac{\partial^2 u}{\partial x^2} - H(x)\frac{\partial u}{\partial x} - H'(x)u\Big)\Big|_k^{n+\theta}, \tag{4}$$

for $k = 2, 3, \ldots, N-1$, and

$$\Big(\frac{\partial}{\partial x}u|_{x=x} - u(x,t)H(x)\Big)\Big|_k^{n+\theta} = 0,$$

for $k = 1, N$, where $n = 1, 2, \ldots, m$.

We denote the numerical solutions of the model at points (k, n), $(k, n+1)$ and $(k, n+\theta)$ by u_k^n, u_k^{n+1} and $u_k^{n+\theta}$, respectively. To describe $u_k^{n+\theta}$ in terms of u_k^n and u_k^{n+1}, we consider the θ-weighted average of the time levels n and $n+1$ for the approximation of right-hand side terms of (4) [8]; that is, the approximation

$$\begin{aligned}\big(\frac{\partial^2 u}{\partial x^2}\big)\big|_k^{n+\theta} &= (1-\theta)\big(\frac{\partial^2 u}{\partial x^2}\big)\big|_k^n + \theta\big(\frac{\partial^2 u}{\partial x^2}\big)\big|_k^{n+1} \\ &= \frac{1}{(\Delta x)^2}\big((1-\theta)(u_{k+1}^n - 2u_k^n + u_{k-1}^n) \\ &\quad + \theta(u_{k+1}^{n+1} - 2u_k^{n+1} + u_{k-1}^{n+1})\big),\end{aligned} \tag{5}$$

for $\big(\frac{\partial^2 u}{\partial x^2}\big)\big|_k^{n+\theta}$, the approximation

$$\begin{aligned}\big(H(x)\frac{\partial u}{\partial x}\big)\big|_k^{n+\theta} &= (1-\theta)\big(H(x)\frac{\partial u}{\partial x}\big)\big|_k^n + \theta\big(H(x)\frac{\partial u}{\partial x}\big)\big|_k^{n+1} \\ &= \frac{H_k}{2\Delta x}\big((1-\theta)\big((u_{k+1}^n - u_k^n)\big) + \theta(u_{k+1}^{n+1} - u_k^{n+1})\big),\end{aligned} \tag{6}$$

for $\big(H(x)\frac{\partial u}{\partial x}\big)\big|_k^{n+\theta}$ and

$$\big(H'(x)u\big)\big|_k^{n+\theta} = (1-\theta)\big(H'(x)u\big)\big|_k^n + \theta\big(H'(x)u\big)\big|_k^{n+1}, \tag{7}$$

for $\big(H'(x)u\big)\big|_k^{n+\theta}$. To approximate the time derivative $\big(\frac{\partial u}{\partial t}\big)\big|_k^{n+\theta}$, we have

$$u_k^n = u_k^{n+\theta} - \theta\Delta t\big(\frac{\partial u}{\partial t}\big)\big|_k^{n+\theta} + \theta^2\frac{(\Delta t)^2}{2}\big(\frac{\partial^2 u}{\partial t^2}\big)\big|_k^{n+\theta} - \theta^3\frac{(\Delta t)^3}{6}\big(\frac{\partial^3 u}{\partial t^3}\big)\big|_k^{n+\theta} + \ldots,$$

and

$$\begin{aligned}u_k^{n+1} &= u_k^{n+\theta} + (1-\theta)\Delta t\big(\frac{\partial u}{\partial t}\big)\big|_k^{n+\theta} + (1-\theta)^2\frac{(\Delta t)^2}{2}\big(\frac{\partial^2 u}{\partial t^2}\big)\big|_k^{n+\theta} \\ &\quad + (1-\theta)^3\frac{(\Delta t)^3}{6}\big(\frac{\partial^3 u}{\partial t^3}\big)\big|_k^{n+\theta} + \ldots.\end{aligned}$$

Therefore

$$\begin{aligned}u_k^{n+1} - u_k^n &= (1-\theta+\theta)\Delta t\big(\frac{\partial u}{\partial t}\big)\big|_k^{n+\theta} + (1-2\theta)\frac{(\Delta t)^2}{2}\big(\frac{\partial^2 u}{\partial t^2}\big)\big|_k^{n+\theta} \\ &\quad + (3\theta^2 - 3\theta + 1)\frac{(\Delta t)^3}{6}\big(\frac{\partial^3 u}{\partial t^3}\big)\big|_k^{n+\theta} + \ldots.\end{aligned}$$

Hence

$$\big(\frac{\partial u}{\partial t}\big)\big|_k^{n+\theta} = \frac{u_k^{n+1} - u_k^n}{\Delta t} + O\big((\Delta t)^p\big), \tag{8}$$

where $p = 3$ if $\theta = \frac{1}{2}$, and $p = 2$ if $\theta \neq \frac{1}{2}$.

We substitute Eqs. (5)-(8) in (4) and we have

$$\begin{aligned}\frac{u_k^{n+1} - u_k^n}{\Delta t} = \ & \mathcal{K}\Big[\frac{1}{(\Delta x)^2}\big((1-\theta)(u_{k+1}^n - 2u_k^n + u_{k-1}^n) \\ & + \theta(u_{k+1}^{n+1} - 2u_k^{n+1} + u_{k-1}^{n+1})\big) \\ & - H_k\Big(\frac{1}{2\Delta x}\big((1-\theta)(u_{k+1}^n - u_{k-1}^n) + \theta(u_{k+1}^{n+1} - u_{k-1}^{n+1})\big)\Big) \\ & - \big((1-\theta)H_k' u_k^n + \theta H_k' u_k^{n+1}\big)\Big].\end{aligned}$$

A simple calculation yields

$$\begin{aligned}& u_k^{n+1} - \frac{\mathcal{K}\Delta t}{(\Delta x)^2}\theta(u_{k+1}^{n+1} - 2u_k^{n+1} + u_{k-1}^{n+1}) + \frac{\mathcal{K}\Delta t}{2\Delta x}\theta H_k(u_{k+1}^{n+1} - u_{k-1}^{n+1}) \\ & + \mathcal{K}\Delta t\theta H_k' u_k^{n+1} = u_k^n + \frac{\mathcal{K}\Delta t}{(\Delta x)^2}(1-\theta)(u_{k+1}^n - 2u_k^n + u_{k-1}^n) \\ & - \frac{\mathcal{K}\Delta t}{2\Delta x}(1-\theta)H_k(u_{k+1}^n - u_{k-1}^n) - \mathcal{K}\Delta t(1-\theta)H_k' u_k^n.\end{aligned} \tag{9}$$

In the above equation, by assigning 0, $\frac{1}{2}$, and 1 to θ, the resulting equations are equivalent to backward difference, Crank-Nicolson, and forward difference methods, respectively.

Also, we apply the following backward and forward differences for the boundary conditions at the points $x = 0$ and $x = 1$, respectively, as

$$\begin{aligned}\frac{(1-\theta)(u_2^n - u_1^n) + \theta(u_2^{n+1} - u_1^{n+1})}{\Delta x} &= (1-\theta)H_1 u_1^n + \theta H_1 u_1^{n+1}, \\ \frac{(1-\theta)(u_N^n - u_{N-1}^n) + \theta(u_N^{n+1} - u_{N-1}^{n+1})}{\Delta x} &= (1-\theta)H_N u_N^n + \theta H_N u_N^{n+1}.\end{aligned} \tag{10}$$

3 Stability analysis

For the stability analysis, we utilize the Von Neumann method based on the Fourier series. Based on this method, the initial cells are written as a finite summation. Then the method considers the growth of a function

reduced by a "variables separable" for the summation [8]. According to that, we set $u_k^n = e^{i\beta x_k}\xi^n$ with $i^2 = -1$, in Eq. (9) and then

$$\begin{aligned}
&e^{i\beta x_k}\xi^{n+1} - \frac{\mathcal{K}\Delta t}{(\Delta x)^2}\theta(e^{i\beta x_{k+1}}\xi^{n+1} - 2e^{i\beta x_k}\xi^{n+1} + e^{i\beta x_{k-1}}\xi^{n+1}) \\
&+ \frac{\mathcal{K}\Delta t}{2\Delta x}\theta H_k(e^{i\beta x_{k+1}}\xi^{n+1} - e^{i\beta x_{k-1}}\xi^{n+1}) + \theta H_k' e^{i\beta x_k}\xi^{n+1} \\
=&e^{i\beta x_k}\xi^n + \frac{\mathcal{K}\Delta t}{(\Delta x)^2}(1-\theta)(e^{i\beta x_{k+1}}\xi^n - 2e^{i\beta x_k}\xi^n + e^{i\beta x_{k-1}}\xi^n) \\
&- \frac{\mathcal{K}\Delta t}{2\Delta x}(1-\theta)H_k(e^{i\beta x_{k+1}}\xi^n - e^{i\beta x_{k-1}}\xi^n) - (1-\theta)H_k' e^{i\beta x_k}\xi^n.
\end{aligned}$$

So

$$\begin{aligned}
&\xi\big[1 - \frac{\mathcal{K}\Delta t}{(\Delta x)^2}\theta(e^{i\beta\Delta x} - 2 + e^{-i\beta\Delta x}) + \frac{\mathcal{K}\Delta t}{2\Delta x}\theta H_k(e^{i\beta\Delta x} - e^{-i\beta\Delta x}) + \theta H_k'\big] \\
&= 1 + \frac{\mathcal{K}\Delta t}{(\Delta x)^2}(1-\theta)(e^{i\beta\Delta x} - 2 + e^{-i\beta\Delta x}) \\
&\quad - \frac{\mathcal{K}\Delta t}{2\Delta x}(1-\theta)H_k(e^{i\beta\Delta x} - e^{-i\beta\Delta x}) - (1-\theta)H_k'.
\end{aligned}$$

Then, the method discussed in Eq. (9) is stable if and only if $|\xi| \le 1$ [8]. By a simple calculation, this condition yields

$$\frac{1}{2} - \frac{\frac{4\mathcal{K}\Delta t}{(\Delta x)^2}\sin^2\frac{\beta\Delta x}{2} + \mathcal{K}\Delta t H_k'}{\big(\frac{4\mathcal{K}\Delta t}{(\Delta x)^2}\sin^2\frac{\beta\Delta x}{2} + \mathcal{K}\Delta t H_k'\big)^2 + \big(\frac{\mathcal{K}\Delta t}{\Delta x}H_k\sin(\beta\Delta x)\big)^2} \le \theta \le 1. \qquad (11)$$

Therefore, by choosing values of $\mathcal{K}$, Δt and Δx satisfying in Eq. (11), the FD method for Eq. (4) will be stable. Also Eq. (11) shows that the FD method can be extensively applied for solving the model by more extensive values of $\mathcal{K}$.

4 Numerical simulations

Now, some numerical cases for the presented model are studied. Each case investigates the change effect of one or more parameters. To have a comparison, we put $a = 0.1$, $b = 2$, $e = 10$, $\beta_1 = \beta_2 = 1$, $A = 28 \times 10^7$ and $B = 22 \times 10^9$ like [1,2,6,7].

We cannot compare the solution directly because of the unavailability of the exact solution of (1). Therefore, to explain the accuracy and efficiency

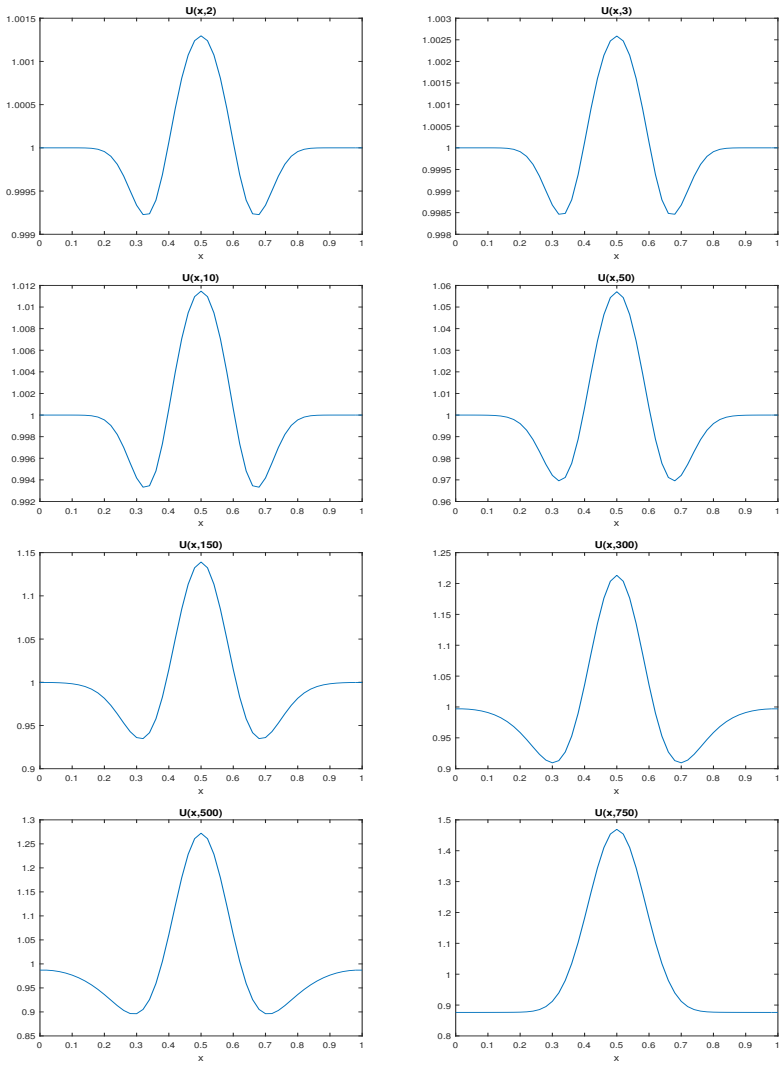

Figure 1: Numerical results of case 4.1.

of the method, we define a pointwise approximate relative error as

$$\varepsilon = \sqrt{\frac{\sum_{i=1}^{N}(u^n_{\tilde{i},\tilde{N}} - u^n_{i,N})^2}{\sum_{i=1}^{N}(u^n_{\tilde{i},\tilde{N}})^2}}.$$

In the above equation, $u^n_{i,N}$ and $u^n_{\tilde{i},\tilde{N}}$ are the approximation solutions for Eqs. (9)-(10) by partitioning of the spatial domain at level n by N, and $\tilde{N}$

Table 1: Relative error and L_∞ for Case 4.1.

t	Relative error $\tilde{N} = 2N - 1$	Relative error $\tilde{N} = 2N - 3$	$L_\infty = \|u_{n+1} - u_n\|_\infty$
0.5	2.9166×10^{-7}	3.6559×10^{-6}	1.2633×10^{-3}
10	1.2465×10^{-6}	1.5616×10^{-3}	1.2359×10^{-3}
50	2.1096×10^{-5}	2.6381×10^{-6}	1.0201×10^{-3}
100	5.9114×10^{-5}	7.3900×10^{-5}	7.9938×10^{-4}
300	2.3557×10^{-4}	2.9549×10^{-4}	3.7545×10^{-4}
500	3.9661×10^{-4}	5.0514×10^{-4}	2.2954×10^{-4}
600	4.7300×10^{-4}	6.0813×10^{-4}	1.8987×10^{-4}
750	5.8349×10^{-4}	7.5986×10^{-4}	1.4933×10^{-4}

—

Table 2: A comparison between FD and RBF methods for Case 4.1.

t	Relative error FD method	Relative error RBF method	Difference
1	0	2.0893×10^{-6}	2.0893×10^{-6}
2	2.5790×10^{-8}	3.1839×10^{-3}	3.1839×10^{-3}
10	1.2465×10^{-6}	4.5941×10^{-6}	3.3476×10^{-6}
50	2.1096×10^{-5}	3.5833×10^{-6}	1.7513×10^{-5}
100e	5.9114×10^{-5}	1.1834×10^{-5}	4.7280×10^{-5}
200	1.4812×10^{-4}	1.1015×10^{-5}	1.3710×10^{-4}
375	2.9769×10^{-4}	1.6142×10^{-5}	2.8155×10^{-4}
500	3.9661×10^{-4}	3.3619×10^{-5}	3.6299×10^{-4}
600	4.7300×10^{-4}	4.8475×10^{-5}	4.2452×10^{-4}
750	5.8349×10^{-4}	7.1250×10^{-5}	5.1224×10^{-4}

points, respectively, such that x_i in N-point partition is the same as $x_{\tilde{i}}$ in the $\tilde{N}$-point partition. For this purpose, we choose $\tilde{\gamma} = 2\gamma - 1$ or $\tilde{\gamma} = 4\gamma - 3$ for $\gamma = N, i$.

All solutions obtained by starting with the initial cells, and then used the iterated method mentioned in Eqs. (9)-(10).

4.1 Case 1

In the first case, we consider the problem (1) with $\mathcal{K} = 0.00025$ as the cell diffusion constant and $\tau = 750$. The proposed approach is performed

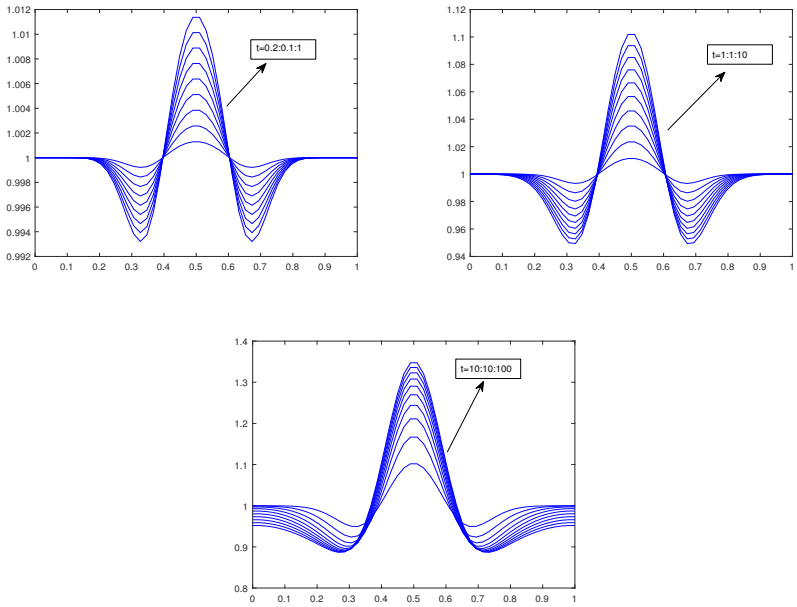

Figure 2: Numerical results of case 4.2

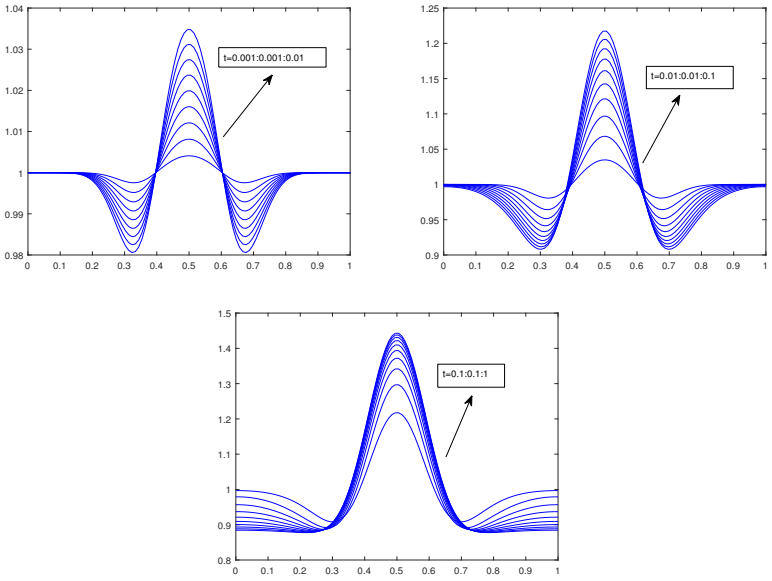

Figure 3: Numerical results of case 4.3.

Table 3: Relative error and L_∞ for Case 4.2.

t	Relative error $\tilde{N} = 2N - 1$	Relative error $\tilde{N} = 4N - 3$	$L_\infty = \|u_{n+1} - u_n\|_\infty$
0.05	3.1431×10^{-9}	8.7349×10^{-5}	1.2860×10^{-4}
0.1	1.4489×10^{-8}	2.3549×10^{-4}	1.2833×10^{-4}
0.5	3.7478×10^{-7}	1.4241×10^{-3}	1.2616×10^{-4}
1	1.3944×10^{-6}	2.8807×10^{-3}	1.2341×10^{-4}
3	9.5523×10^{-6}	8.3880×10^{-3}	1.1236×10^{-4}
5	2.1485×10^{-5}	1.3440×10^{-2}	1.0182×10^{-4}
6	2.8337×10^{-5}	1.5815×10^{-2}	9.6886×10^{-5}
7.5	3.9446×10^{-5}	1.9208×10^{-2}	8.9978×10^{-5}
9	5.1353×10^{-5}	2.2414×10^{-2}	8.3671×10^{-5}
10	5.9640×10^{-5}	2.4457×10^{-2}	7.9792×10^{-5}

Table 4: Relative error and L_∞ for Case 4.3.

t	Relative error $\tilde{N} = 2N - 1$	Relative error $\tilde{N} = 2N - 3$	$L_\infty = \|u_{n+1} - u_n\|_\infty$
0.005	7.4011×10^{-7}	9.2545×10^{-7}	3.8622×10^{-3}
0.01	2.4845×10^{-6}	3.1062×10^{-6}	3.5812×10^{-3}
0.05	2.7170×10^{-5}	3.3982×10^{-5}	1.9700×10^{-3}
0.1	6.2807×10^{-5}	7.9604×10^{-5}	1.1340×10^{-3}
0.3	2.3174×10^{-4}	3.2360×10^{-4}	3.5874×10^{-4}
0.5	3.6314×10^{-4}	5.1724×10^{-4}	1.8537×10^{-4}
0.6	4.0280×10^{-4}	5.7536×10^{-4}	1.3839×10^{-4}
0.75	4.3812×10^{-4}	6.2664×10^{-4}	9.0302×10^{-5}
0.9	4.5399×10^{-4}	6.4870×10^{-4}	5.9266×10^{-5}
1	4.5789×10^{-4}	6.5308×10^{-4}	4.4860×10^{-5}

using $N = 50$, $\Delta t = 0.1$ and $\theta = \frac{1}{2}$ (the Crank-Nicolson finite difference method). Figure 1 shows the results of the method for this case which are like the results of [1, 2, 6, 7]. Also, Table 1 shows the relative error and $L_\infty = \|u_{n+1} - u_n\|_\infty$ for this Case. As seen, the L_∞ is decreased by growing the time level, while the L_∞ was significantly surged in the RBF method as the shape parameter increased [1]. Moreover, Table 2 shows a comparison between the FD and RBF methods for Case 4.1.

Note that the RBF method was stable for the only multiquadric function

and a few values of its shape parameter, which has not appeared in the method.

4.2 Case 2

In this case, we set the problem with $\tau = 100$, $\Delta t = 0.01$ and the other parameter like Case 4.1. Table 3 relates some relative error and Figure 2 shows some results of this case. Similar to Case 4.1, the L_∞ error has decreased.

4.3 Case 3

As the third and last case, we put $N = 100$, $\mathcal{K} = 0.08$, $\tau = 1$, $\Delta t = 0.001$ and $\theta = 1$ for Eq. (9). Table 4 and Figure 3 present the results of the third case.

5 Conclusion and comments

In this study, the finite difference method was applied for a mathematical model of capillary formation in the angiogenesis tumor by discretizing of two successive levels of time, called the θ-method. Then the stability of the method was discussed based on the Von Neumann method which yields the convergence according to Lax's theorem [8]. In order to demonstrate the correction of this stability, several numerical cases were simulated, in which the change of the cell diffusion constant, as well as the variations of different parameters of the numerical method were used to obtain the approximated solution at different time levels.

References

[1] S. Abbasbandy, H.G. Roohani and I. Hashim, *Numerical analysis of a mathematical model for capillary formation in tumor angiogenesis using a mesh free method based on the radial basis function*, Engineering Analysis with Boundary Elements **36** (2012) 1811-1818.

[2] N. Gucuyenen and G. Tanoglu, *Iterative operator splitting method for capillary formation model in tumor angiogenesis problem: analysis and application*, Int. J. Numer. Meth. Biomed. Eng. **27** (2011) 1740-1750.

[3] A. Khodadadian, K. Hosseini and A. Ali Manzour-Ol-Ajdad, M. Hedayati, R. Kalantarinejad, C. Heitzinger, *Optimal design of nanowire field-effect troponin sensors*, Comput. Biol. Med. **87** (2017) 46-56.

[4] A. Khodadadian and C. Heitzinger, *A transport equation for confined structures applied to the OprP, Gramicidin A, and KcsA channels*, J. Comput. Electron. **14**(2) (2015) 524-532.

[5] H.A. Levine, S. Pamuk, B.D. Sleeman and M. Nilsen-Hamilton, *Mathematical model of capillary formation and development in tumor angiogenesis: penetration into the stroma*, Bull. Math. Biol. **63**(5) (2001) 801-863.

[6] S. Pamuk and A. Endern, *The method of lines for the numerical solution of a mathematical model for capillary formation: the role of endothelial cells in the capillary*, Appl. Math. Comput. **186** (2007) 831-835.

[7] A. Saadatmandi and M. Dehghan, *Numerical solution of a mathematical model for capillary formation in tumor angiogenesis via the tau method*, Commun. Numer. Math. Engng. **24** (2008) 1467-1474.

[8] G.D. Smith, *Numerical solution of partial differential equations*, Third Edition, Clarendon Press, Oxford, 1985.